IMECE2012-87547

DEVIATIONAL PHONONS AND THERMAL TRANSPORT AT THE NANOSCALE

Jean-Philippe M. Péraud
Department of Mechanical Engineering
Massachusetts Institute of Technology
Cambridge, MA 02139, USA
Email: jperaud@mit.edu

Nicolas G. Hadjiconstantinou
Department of Mechanical Engineering
Massachusetts Institute of Technology
Cambridge, MA 02139, USA
Email: ngh@mit.edu

ABSTRACT

We present a new method for simulating phonon transport at the nanoscale. The proposed approach is based on the recently developed energy-based deviational Monte Carlo method by the authors [Phys. Rev. B 84, 205331, 2011] which achieves significantly reduced statistical uncertainty compared to standard Monte Carlo methods by simulating only the deviation from equilibrium. Here, we show that under linearized conditions (small temperature differences) the trajectories of individual particles simulating the deviation from equilibrium can be decoupled and can thus be simulated independently, without introducing any additional approximation. This leads to a particularly simple and efficient simulation method that can be used to treat steady and transient phonon transport problems in arbitrary three-dimensional geometries.

INTRODUCTION

We present an efficient method for solving the Boltzmann transport equation (BTE) for phonons in the relaxation-time approximation, as needed, for example, for describing transport at scales that are sufficiently small that Fourier's law is no longer valid, but sufficiently large to be out of the reach of molecular simulation methods. The proposed approach belongs to a new class of methods, referred to as deviational, in which computational particles simulate only the deviation from an appropriately chosen equilibrium distribution, while the contribution of the equilibrium component of the distribution is provided analytically.

Deviational methods were originally proposed as control-variate variance-reduction formulations for solving the Boltzmann equation in the context of nanoscale gas flows [1]. In a recent publication [2], the authors developed a deviational method for simulating phonon transport which exhibits substantial computational speedup compared to traditional Monte Carlo methods in the limit of small temperature differences. As shown in [2], this feature, coupled with the ability of deviational methods to focus the computational effort in regions where it is most needed, has enabled the simulation of complex multiscale problems that would otherwise be intractable.

In the present article we show that problems for which the BTE can be linearized can be solved by a new method in which deviational computational particles can be treated as non-interacting. This results in a simulation algorithm that is simpler, does not use any approximation in space or time, and depending on the application of interest, can be several orders of magnitude faster than the one described in [2].

DEVIATIONAL APPROACH

The deviational approach [1–5] starts by writing the BTE in terms of the deviation from equilibrium $f^d = f - f^{eq}_{T_{eq}}$ in the form

$$\frac{\partial f^d}{\partial t} + \mathbf{V}_g \cdot \nabla f^d = \frac{(f^{loc} - f^{eq}_{T_{eq}}) - f^d}{\tau} \qquad (1)$$

where $\tau = \tau(\omega, p, T)$ is the relaxation time, $f = f(\mathbf{x}, \omega, p, \theta, \phi)$ is the occupation number of phonon states, $\mathbf{V}_g$ is the phonon-bundle group velocity and $f^{eq}_{T_{eq}}$ is a Bose-Einstein distribution at

the "control" temperature T_{eq}, namely

$$f^{eq}_{T_{eq}} = \frac{1}{\exp\left(\frac{\hbar\omega}{k_b T_{eq}}\right) - 1} \qquad (2)$$

For phonon transport in particular, the authors have shown [2] that the energy conserving properties of the simulation algorithm are significantly improved if, instead, the following energy-based BTE

$$\frac{\partial e^d}{\partial t} + \mathbf{V}_g \cdot \nabla e^d = \frac{(e^{loc} - e^{eq}_{T_{eq}}) - e^d}{\tau} \qquad (3)$$

is simulated, where $e^d = \hbar\omega f^d$. Deviational methods reduce the computational cost by simulating only the distribution De^d ($D = D(\omega, p)$ is the density of states) using deviational particles, because the contribution of $De^{eq}_{T_{eq}}$ is known analytically. The key to creating deviational algorithms is to realize that (3) suggests that during the scattering step, particles from the distribution De^d/τ are removed and replaced by new particles with random traveling directions and properties (frequency and polarization) drawn from $D(e^{loc} - e^{eq}_{T_{eq}})/\tau$. In the following, we present an improvement to this general simulation procedure that leads to significant computational savings for problems where the BTE can be linearized.

PROPOSED METHOD

For small temperature differences, the BTE can be linearized to yield

$$\frac{\partial e^d}{\partial t} + \mathbf{V}_g \cdot \nabla e^d = \frac{\mathcal{L}(e^d) - e^d}{\tau_{eq}} \qquad (4)$$

where the particle generation term of the collision operator in (3) can now be written in the form

$$\mathcal{L}(e^d) = \frac{de^{eq}_{T_{eq}}}{dT}(T_{loc} - T_{eq}) \qquad (5)$$

and $\tau_{eq} = \tau(\omega, p, T_{eq})$. As discussed, for example, in [6], T_{loc} is the pseudo-temperature, required in the relaxation time approximation because of the frequency-dependence of the relaxation time $\tau(\omega, p, T)$. Specifically, the pseudo-temperature T_{loc} is defined via the energy conservation statement

$$\int_\omega \left(\sum_p \frac{D(\omega, p)}{\tau_{eq}} \right) \frac{de^{eq}_{T_{eq}}}{dT} \Delta T_{loc} d\omega = \int_\omega \int_\Omega \left(\sum_p \frac{D(\omega, p) e^d}{4\pi\tau_{eq}} \right) d\Omega d\omega \qquad (6)$$

which implies

$$\Delta T_{loc} = \left[\int_\omega \int_\Omega \sum_p \frac{De^d}{4\pi\tau_{eq}} d\Omega d\omega \bigg/ \int_\omega \sum_p \frac{D}{\tau_{eq}} \frac{de^{eq}_{T_{eq}}}{dT} d\omega \right] \qquad (7)$$

where $de^{eq}_{T_{eq}}/dT$ can be calculated analytically from the Bose-Einstein distribution.

In [2], we exploited this form of the collision operator to avoid sampling the local temperature in the far field where deviational temperatures were small: because the distribution

$$(T_{loc} - T_{eq}) \frac{D(\omega, p)}{\tau(\omega, p, T_{eq})} \frac{de^{eq}_{T_{eq}}}{dT} \qquad (8)$$

does not depend on $(T_{loc} - T_{eq})$ *once normalized*, a particle which undergoes a scattering event (at rate τ_{eq}) can be drawn from (the normalized form of) this distribution without requiring any information on the local value of T_{loc}, while energy conservation is simply ensured by conserving the particle.

Using this formulation throughout the computational domain results in considerable benefits: since knowledge of T_{loc} is no longer needed for the scattering process, computational particles can be considered as behaving independently. Hence, trajectories are no longer integrated collectively; instead, they are simulated sequentially, which requires significantly less storage. Furthermore, integration timesteps and computational cells as used in standard Monte Carlo approaches [7] are no longer needed. Instead, for each independent particle trajectory, the time between scattering events can be computed directly from (4) thus avoiding the numerical error associated with timestep based integration methods. This contributes significantly to reducing the number of operations between scattering events and, depending on the problem of interest, the resulting algorithm is several orders of magnitude more computationally efficient.

The proposed algorithm for calculating an individual particle trajectory from $t = 0$ to $t = t_f$ is described below. Note that in the interest of simplicity we have suppressed the particle index i.

I Draw the initial properties (sign s, position $\mathbf{x}_0$, frequency ω_0, polarization p_0, direction Ω_0, and the resulting group velocity vector $\mathbf{V}_{g,0}$) of the particle. For time-dependent calculations, also set up the initial time t_0 of the particle; this is discussed in more detail below.

II Calculate the traveling time until the first scattering (relaxation) event, Δt. Times between scattering events are drawn from a decaying exponential with mean lifetime τ. This is implemented by uniformly drawing a random number R between 0 and 1, and setting

$$\Delta t = -\tau(\omega_0, p_0, T_{eq}) \ln(R) \qquad (9)$$

III Calculate $\tilde{\mathbf{x}}_{new} = \mathbf{x}_0 + \mathbf{V}_{g,0}\Delta t$. Search for collisions with system boundaries along the line $[\mathbf{x}_0, \tilde{\mathbf{x}}_{new}]$.

IVa If a collision with a system boundary occurs, say at $\mathbf{x}_b$, set $\mathbf{x}_{new} = \mathbf{x}_b$ and update the internal time $t_{new} = t_0 + ||(\mathbf{x}_b - \mathbf{x}_0)||/||\mathbf{V}_{g,0}||$. Depending on the nature of the reflection (specular or diffuse), set the new traveling direction appropriately (as explained for example in [8]).

IVb If no collision with system boundaries occurs, the particle undergoes scattering at position $\mathbf{x}_{new} = \tilde{\mathbf{x}}_{new}$. The internal time is updated to $t_{new} = t_0 + \Delta t$. New frequency ω_{new} and polarization p_{new} are then drawn from the distribution (8). A new traveling direction is also chosen: in this work, we consider isotropic scattering, but this can easily be generalized to non-isotropic scattering. From these parameters, a new velocity vector $\mathbf{V}_{g,new}$ can be defined. The particle sign remains unchanged by scattering.

V The contribution of segment $[\mathbf{x}_0, \mathbf{x}_{new}]$ to macroscopic properties is sampled. Sampling is discussed in more detail below.

VI If $t_{new} > t_f$, proceed to step I to begin simulation of the next particle; otherwise, set $\{.\}_0 = \{.\}_{new}$, where $\{.\}$ denotes the set of all properties of particle i, and return to step II.

The total number of particles processed, N, can be chosen arbitrarily, depending on the desired statistical uncertainty. From this choice, the effective energy carried by each computational particle, $\mathcal{E}_{eff}$, can be calculated as the total amount of deviational energy involved in the phenomenon of interest divided by N. The total deviational energy includes the magnitude of the deviational energy present in the initial condition $MDE_{ic} = \sum_p \int_{\mathbf{x},\omega,\Omega} (4\pi)^{-1}D|e^d(t=0)|d\mathbf{x}d\omega d\Omega$, as well as the magnitude of the deviational energy associated with boundary conditions or other source terms over the course of the simulation; the former will be denoted here as $MDE_{bc} = \sum_p \int_{t'=0}^{t_f} \int_{\mathbf{S},\omega,\Omega \in \mathbf{V}_g \cdot \hat{\mathbf{n}} > 0} (4\pi)^{-1}D\mathbf{V}_g \cdot \hat{\mathbf{n}}|e^d|d\mathbf{x}d\omega d\Omega dt'$, where $\mathbf{S}$ denotes the surface area and $\hat{\mathbf{n}}$ the surface normal of the boundary, while the latter will be denoted by $MDE_s = \sum_p \int_{t'=0}^{t_f} \int_{\mathbf{x},\omega,\Omega} (4\pi)^{-1}D|\dot{e}_s^d|d\mathbf{x}d\omega d\Omega dt'$; concrete examples of these quantities will be given below. The number of particles associated with MDE_i where $i \in \{ic,bc,s\}$ is given by $MDE_i N/(MDE_{ic} + MDE_{bc} + MDE_s)$. The initial time for particles due to the initial condition is set to $t_0 = 0$, while t_0 for the remaining particles is drawn randomly in the interval $[0,t_f]$ and proportionally to the rate of deviational energy input/removal from the simulation (e.g. for a source term, this can be achieved by inverting the cumulative distribution function given by the absolute value of the deviational energy input/removal function $\sum_p \int_{t'=0}^{t} \int_{\mathbf{x},\omega,\Omega} (4\pi)^{-1}D|\dot{e}_s^d|d\mathbf{x}d\omega d\Omega dt'$).

Let us illustrate these concepts with a 1D example, namely, transient heat transfer between two walls at fixed and different temperatures [9]; the walls are located at $X = 0$ and $X = L$, and their temperatures are T_1 and T_2, respectively. In order to illustrate the implementation of initial conditions, we take the initial system temperature to be

$$T_0(X) = \frac{T_1 + T_2}{2} + \frac{T_1 - T_2}{2}\sin\left(\frac{\pi X}{L}\right) \qquad (10)$$

For $|T_1 - T_2| \ll (T_1 + T_2)/2$, deviations from a *suitably chosen* equilibrium temperature will be small. For example, an obvious choice, is $T_{eq} = (T_1 + T_2)/2$; other equally valid choices are $T_{eq} = T_1$ or $T_{eq} = T_2$. In our calculations, the first possibility, $T_{eq} = (T_1 + T_2)/2$, was used, making the initial condition easier to treat.

The deviational energy terms introduced above reduce to:

$$MDE_{ic} = \int_{X=0}^{L} |T_0(X) - T_{eq}|dX \int_\omega \sum_p D\frac{de_{T_{eq}}^{eq}}{dT}d\omega$$

$$= |T_1 - T_2|\frac{L}{\pi} \int_\omega \sum_p D\frac{de_{T_{eq}}^{eq}}{dT}d\omega$$

$$= |T_1 - T_2|\frac{L}{\pi}C_{T_{eq}} \qquad (11)$$

$$MDE_{bc} = \frac{t_f}{4}\left(|T_1 - T_{eq}| + |T_2 - T_{eq}|\right)\int_\omega \sum_p DV_g\frac{de_{T_{eq}}^{eq}}{dT}d\omega \quad (12)$$

$C_{T_{eq}}$ corresponds to the volumetric specific heat of phonons at temperature T_{eq} [10]. Since no other source terms are introduced in this example, we have $MDE_s = 0$. If a given particle is determined as being emitted from the initial condition, then its initial internal time is $t = 0$, and its initial position (X_0) is randomly drawn between 0 and L according to the spatial distribution of the initial condition, namely

$$P(X) = (T_0(X) - T_{eq})C_{T_{eq}} \qquad (13)$$

which, once normalized and given the expression we chose for T_{eq}, can be written as $p(X) = P(X)/\int_0^L P(X')dX' = \pi(2L)^{-1}\sin(\pi X/L)$. This can, for example, be implemented by drawing a random number R uniformly between 0 and 1 and by setting X_0 such that $R = \int_0^{X_0} p(X)dX$, or $X_0 = L\pi^{-1}\cos^{-1}(1 - 2R)$. If the particle is emitted from the boundary condition, its initial time is uniformly (randomly) drawn between 0 and t_f, while its initial position is either 0 or L depending from which wall it originates. The sign of the emitted particle is determined by the sign of $T_1 - T_{eq}$ and $T_2 - T_{eq}$ at each wall, respectively.

SAMPLING

We now discuss the sampling process in more detail. Let

$$I_g(t) = \sum_p \int_{\mathbf{x},\omega,\Omega} (4\pi)^{-1}Dge^d(t)d\mathbf{x}d\omega d\Omega \qquad (14)$$

be the macroscopic property of interest (at time t) in terms of a general microscopic property $g = g(\mathbf{x}, \omega, p, \Omega)$. Recalling that the deviational simulation approximates the distribution e^d in the phase space using deviational (computational) particles [2]

$$\frac{De^d}{4\pi} \approx \mathcal{E}_{eff} \sum_i s_i \delta^3(\mathbf{x} - \mathbf{x}_i(t)) \delta(\omega - \omega_i(t)) \delta^2(\Omega - \Omega_i(t)) \delta_{p,p_i(t)}, \tag{15}$$

the estimate of $I_g(t)$ is given by

$$\tilde{I}_g(t) = \mathcal{E}_{eff} \sum_i s_i g\left[\mathbf{x}_i(t), \omega_i(t), p_i(t), \Omega_i(t)\right] \tag{16}$$

where symbols have their usual meanings and s_i is the sign of deviational particle i. For example, if the quantity of interest is the X-component of the heat flux vector in some region of space $\mathbf{R}$ with volume $\mu(\mathbf{R})$ and defined by the characteristic function $\chi_{\mathbf{R}}$, then $g = \mathbf{V}_{g,0} \cdot \hat{\mathbf{e}}_X \chi_{\mathbf{R}} / \mu(\mathbf{R})$ and thus particle i only contributes to $I_g(t)$ if $\mathbf{x}_i(t)$ [its position at t—calculated by linear interpolation between (x_0, t_0) and (x_{new}, t_{new})] is in $\mathbf{R}$. The contribution of such a particle to $\tilde{I}_g(t)$ is $s_i[\mathbf{V}_{g,0}]_i \cdot \hat{\mathbf{e}}_X \mathcal{E}_{eff} / \mu(\mathbf{R})$.

As in standard Monte Carlo methods, steady state problems can be sampled by replacing ensemble averaging with time averaging, provided sufficient time has passed for steady conditions to prevail. The proposed method is particularly suited to this type of problem because it can be used to directly solve for the steady state without requiring relaxation of the system from some initial condition, if the latter is of no interest. This can be achieved by including only the steady particle sources (MDE_{bc} and MDE_s) and considering each simulated particle to represent a fixed amount of energy per unit time $\dot{\mathcal{E}}_{eff}$; particles are emitted from the time-independent sources and propagate according to the rules explained above. Since the steady state is constituted of particles at all stages of their time-history, one can sample the values of interest by computing curvilinear integrals along the complete particle trajectories, from their emission to their termination (for example, in a problem with isothermal walls, termination would occur when the particle is absorbed by a boundary). In this case the estimate for $\tilde{I}_g$ is:

$$\tilde{I}_g = \dot{\mathcal{E}}_{eff} \sum_i s_i \int_{\mathbf{x}_i(t) \in \mathbf{R}} g\left[\mathbf{x}_i(t), \omega_i(t), p_i(t), \Omega_i(t)\right] dt \tag{17}$$

The rigorous mathematical proof leading to expressions of this type can be found in linear transport theory literature (see for example [11]) and enables direct sampling of the steady state, contrarily to methods based on timestep. The temperature can for example be calculated by setting $g = (\mu(\mathbf{R})C_{T_{eq}})^{-1}$. Hence, the estimate for the average temperature in a region $\mathbf{R}$ can be

expressed as

$$\tilde{T}_{\mathbf{R}} - T_{eq} = \frac{\dot{\mathcal{E}}_{eff}}{\mu(\mathbf{R})C_{T_{eq}}} \sum_i s_i \int_{\mathbf{x}_i(t) \in \mathbf{R}} dt \tag{18}$$

Although formulations (17) and (18) make use of an internal time for each particle, keeping track of this former parameter in the algorithm explained above is usually made unnecessary by the steady-state nature of the problem. In the case of the temperature (18), one simply needs to compute the total time spent by a given particle in the region $\mathbf{R}$ over its trajectory. In the case of the heat flux in the X-direction ($g = V_X/\mu(\mathbf{R})$) averaged over the domain $\mathbf{R}$, simplifying the integral (17) leads to a time-independent formula:

$$\tilde{J}_{\mathbf{R}} = \frac{\dot{\mathcal{E}}_{eff}}{\mu(\mathbf{R})} \sum_i s_i \mathcal{L}_i \tag{19}$$

where $\mathcal{L}_i$ is the total algebraic length traveled in the X-direction by particle i while in $\mathbf{R}$.

Figure 1 shows both transient and steady state solutions of the one-dimensional problem described above. The steady state solution is obtained as described above, rather than integrating in time from an initial condition. In these simulations, $T_1 = 301\text{K}$, $T_2 = 299\text{K}$, $T_{eq} = 300\text{K}$ leading to an initial condition $T_0(X) = 300 + \sin(\pi X/L)$, while $L = 400\text{nm}$; materials parameters (dispersion relations, scattering rates) are the same as in [2] (Note: phonon-phonon scattering coefficients A_L and A_T given in the appendix A of [2] correspond to a set of units where ω is measured in Hertz. For ω measured in rad/s, they become $A_L = 2.09 \cdot 10^{-19}/(2\pi)^2 = 5.29 \cdot 10^{-21}\text{s/rad}^2/\text{K}^{1.49}$ and $A_T = 1.23 \cdot 10^{-19}/(2\pi)^2 = 3.12 \cdot 10^{-21}\text{s/rad}^2/\text{K}^{1.65}$. The impurity scattering coefficient $A_I = 3 \cdot 10^{-45}\text{s}^3/\text{rad}^4$ and the boundary scattering rate $w_b = 1.2 \cdot 10^6\text{s}^{-1}$ remain unchanged); optical phonons were taken into account (with zero group velocity, as described in [2]).

VALIDATION

The proposed algorithm has been extensively validated using a number of test problems including the thin film problem described in [2] for which an analytical solution exists, and the simple 1D problem mentioned above (Fig. 1), for which the comparison to results calculated with the timestep-based variance-reduced method shows excellent agreement.

The thin film problem (see Fig. 2) can be simulated using the periodic boundary conditions introduced in [6], and deviational particles emitted by boundaries as in [2]. As explained in [2], the hot (resp. cold) boundary at temperature T_1 (resp. T_2) emit
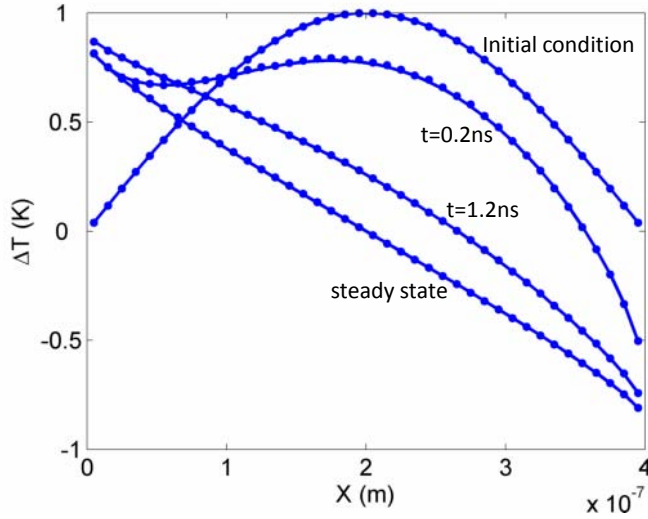
Figure 1. TRANSIENT AND STEADY-STATE TEMPERATURE PRO-FILES BETWEEN TWO WALLS AT $\Delta T = \pm 1K$ AND INITIAL CONDI-TION (10). HERE, $\Delta T = T(X,t) - T_{eq}$ WITH $T_{eq} = 300K$. DOTS: ΔT COMPUTED WITH THE METHOD PRESENTED IN [2]. SOLID LINE: ΔT COMPUTED WITH THE PROPOSED METHOD.

positive (resp. negative) particles according to the distribution

$$-\left(e_{T_1}^{eq} - e_{T_2}^{eq}\right)\frac{D(\omega,p)}{4\pi}V_g(\omega,p)\cos(\theta) \qquad (20)$$

where θ is the angle with respect to the direction of the temperature gradient. This expression can be linearized by writing

$$\left(e_{T_1}^{eq} - e_{T_2}^{eq}\right) \approx (T_1 - T_2)\frac{de_{T_{eq}}^{eq}}{dT} = \frac{de_{T_{eq}}^{eq}}{dT}\frac{dT}{dy}L \qquad (21)$$

While the simulation could be conducted using the 2D model shown in Fig. 2, since we are only interested in the heat flux in the direction along the film ($y-$direction), we can arbitrarily reduce the distance between the two periodic walls while keeping a constant temperature gradient (dT/dy), without modifying the result. In other words, the formulation above is equivalent to simulating particles in a 1D system (variations exist only in the $z-$direction), where the effect of the temperature gradient is accounted for by the volumetric (linear, $0 \le z \le d$) source:

$$-\frac{de_{T_{eq}}^{eq}}{dT}\frac{dT}{dy}\frac{D(\omega,p)}{4\pi}V_g(\omega,p)\cos(\theta) \qquad (22)$$

The signs of the particles are determined by the sign of $\cos(\theta)$. Note that as usual, when drawing the traveling direction of the

particle, the factor $\sin(\theta)$, generally implicit in the expression for the solid angle in spherical coordinate $d\Omega = \sin(\theta)d\theta d\phi$, need to be accounted for (see [8]). Also, note that the factor L does not appear in (22) because the latter describes an emitted power per unit volume, in contrast to (20) which describes an emitted power per unit boundary surface area. This approach of imposing temperature gradients using source terms can be generalized [12] to study transport in periodic nanostructures of arbitrary geometry.

Solution proceeds by using the algorithm explained above over the 1D domain $0 < z < d$, with diffuse reflection at $z = 0$ and $z = d$. However, due to the presence of the source term and the lack of cancellation of deviational particles during the collision step, particle trajectories need to be tracked indefinitely (in contrast to the algorithm presented in [2]). This issue can be circumvented by realizing that the expected value of the heat flux after the first collision with a wall or after the first scattering event is zero because these two types of events randomize the direction of a particle. In other words, because the expected contribution of the trajectory to the heat flux following a scattering event is zero, trajectories can be terminated after their first scattering event. This is verified by Fig. 3; Fig. 4 shows that the resulting simulation method is in good agreement with the theoretical solution for a film of thickness 100nm. The proposed method returns a thermal conductivity of 49.002 ± 0.001 Wm^{-1}K^{-1}. By comparison, numerical integration (via rectangle rule) of the analytical solution presented in [2] returns a thermal conductivity of 48.95 Wm^{-1}K^{-1}.

We emphasize here that terminating deviational trajectories after the first scattering event is only valid for this highly symmetric, 1D problem; a more complete discussion can be found in [12]. The issue of infinite track lengths and a more general criterion for terminating particles in periodic nanostructures is also discussed in [12].

As an application, but also additional validation with our results in [2], we consider the transient thermo-reflectance experiment presented in [13] and used in [14] as a thermal conductivity spectroscopy technique. Using the algorithm described above, we simulate the thermal response of a thin film of aluminum on a substrate of silicon after a laser pulse irradiates the surface and provides localized heating at $t = 0$; the system is initially in equilibrium at $T_0 = 300K$, making this a convenient control temperature, i.e. $T_{eq} = T_0$. Initial positions for the computational particles are determined from the experimentally derived initial temperature distribution

$$T_i - T_0 = (T_1 - T_0)\exp(-\beta z)\exp\left(-\frac{2r^2}{R_0^2}\right), \quad z > 0 \qquad (23)$$

where r represents the radial coordinate measured from the pulse center and z the depth into the aluminum substrate; as previously shown in the transient 1D example above, in the linear
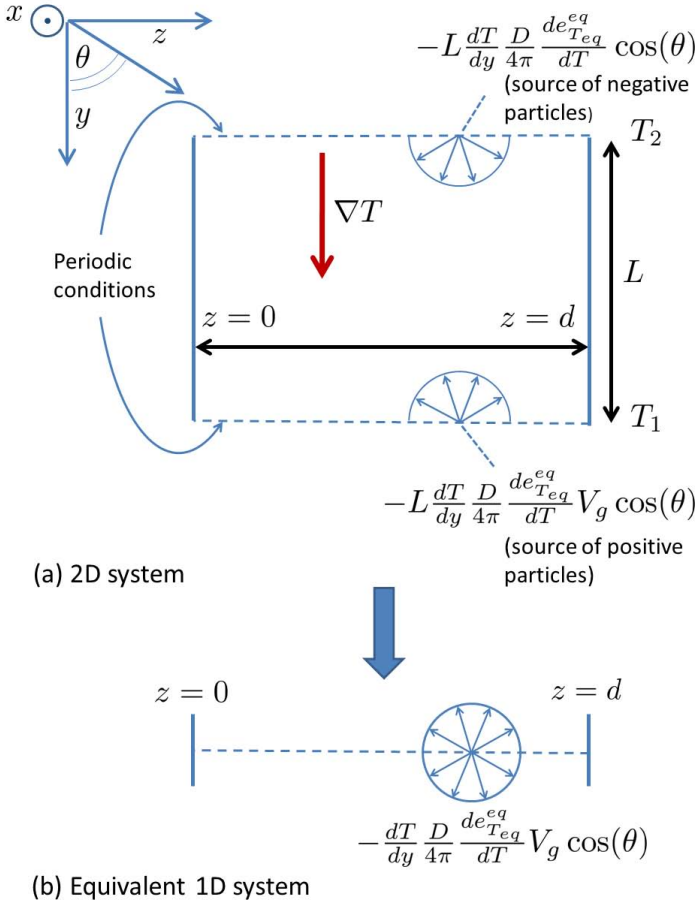
5

$$-L\frac{dT}{dy}\frac{D}{4\pi}\frac{de_{T_{eq}}^{eq}}{dT}\cos(\theta)$$

(source of negative particles)

$$-L\frac{dT}{dy}\frac{D}{4\pi}\frac{de_{T_{eq}}^{eq}}{dT}V_g\cos(\theta)$$

(source of positive particles)

(a) 2D system

$$-\frac{dT}{dy}\frac{D}{4\pi}\frac{de_{T_{eq}}^{eq}}{dT}V_g\cos(\theta)$$

(b) Equivalent 1D system

Figure 2. SIMULATION GEOMETRY. BOUNDARIES AT $z = 0$ AND $z = d$ ARE DIFFUSELY REFLECTING. (a) INFINITE DOMAIN IN THE y-DIRECTION IS TERMINATED BY USE OF PERIODIC BOUNDARIES SEPARATED BY A DISTANCE L. (b) REDUCED SIMULATION GEOMETRY.

approximation we can draw the initial properties of the deviational particles from a distribution that is proportional to the initial temperature distribution, or in other words $e^d(\mathbf{x}, \omega, \Omega, t = 0) \propto (T_i(\mathbf{x}) - T_0)de_{T_{eq}}^{eq}/dT$. Also, since the heating is impulsive in time, each particle's initial time is set to $t = 0$. Particle trajectories are calculated with the procedure explained above.

The Al/Si interface is treated as follows: the probability of a deviational particle crossing or being reflected at the interface is calculated using the frequency dependent interface condition detailed in [15,16]. When a particle trajectory intersects the interface, the particle is transmitted or reflected by comparing the transmission/reflection probability with a uniformly drawn random number. In case of crossing, a new traveling time until the next scattering event needs to be calculated using (9) and the parameters of the new traveling medium. Reflection is treated as
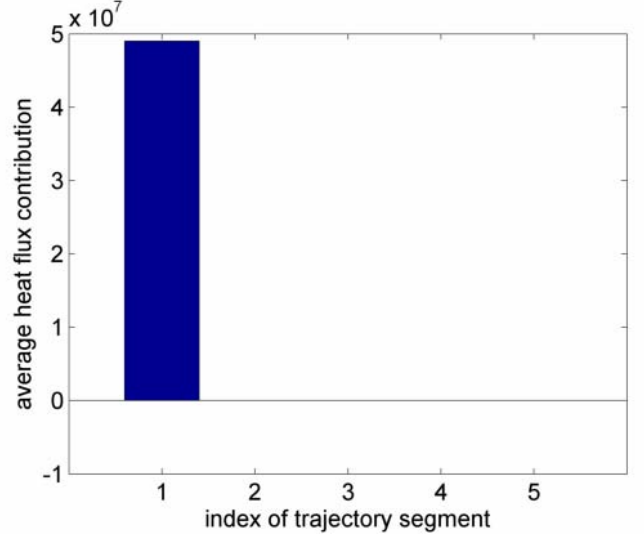

Figure 3. AVERAGE HEAT FLUX CONTRIBUTIONS (Wm^{-2}) BE-TWEEN THE $(j-1)$-TH AND THE j-TH SCATTERING EVENT, FOR THE CALCULATION OF THE THERMAL CONDUCTIVITY ALONG A THIN FILM. AFTER THE FIRST COLLISION, THE EXPECTED HEAT FLUX IS ZERO.

algorithm item [IVa] discussed above. These calculations used $T_1 = 301$K, $\beta^{-1} = 7$nm, $R_0 = 15\mu$m and the same materials parameters as in [2].

Figure 5 shows that the proposed method yields results that are in excellent agreement with the deviational method presented in [2]. However, the *additional* speedup due to the present algorithm allows us to calculate the response to a single pulse up to 10μs [12], which represents a two to three order of magnitude improvement compared to the deviational method presented in [2] which could only reach several nanoseconds. (For comparison purposes, we note that due to the small temperature differences involved, simulation of this problem using standard Monte Carlo methods is essentially intractable.) Ultimately, we expect this improvement to be invaluable towards the computational description of the phonon spectroscopy experiment discussed in [14].

CONCLUSIONS

We have presented a new method for simulating phonon transport at the nanoscale valid for problems exhibiting sufficiently small deviations from equilibrium that the BTE can be linearized. Although the exact range of temperatures under which linearization is valid depends on the error that can be tolerated, we expect linearization to be appropriate for $\Delta T/T_{eq} \lesssim 0.1$; for $T_{eq} \sim 300$K, this translates to a requirement that $\Delta T \lesssim 30$K, which is satisfied by a wide range of applications of current interest. Provided linearization is appropriate, in addition to improved
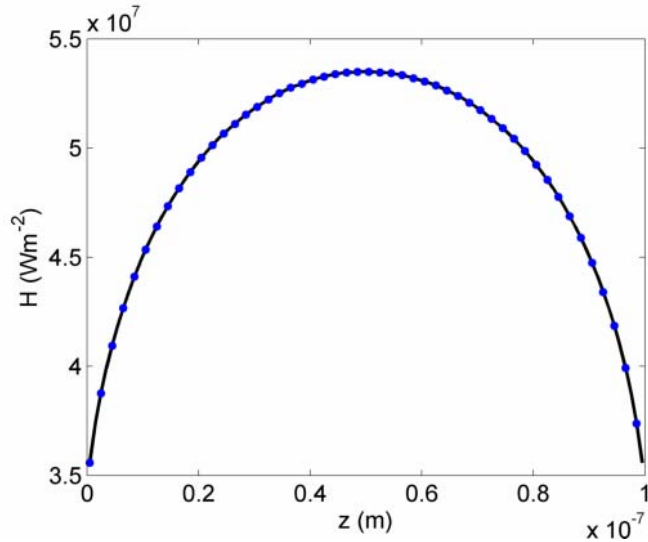
6

Figure 4. VALIDATION OF THE PROPOSED ALGORITHM. SOLID LINE: THEORETICAL HEAT FLUX IN A THIN FILM OF THICKNESS 100nm. DOTS: HEAT FLUX COMPUTED WITH THE PROPOSED METHOD.
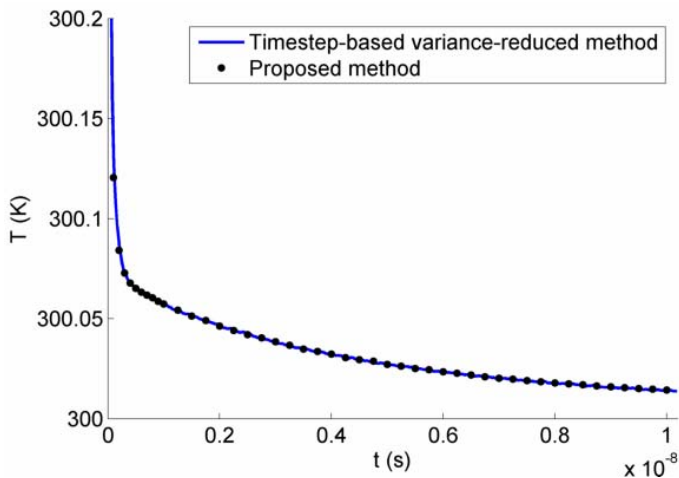

Figure 5. COMPARISON OF THE SURFACE TEMPERATURE (AVERAGED OVER A DEPTH OF 5nm IN A CYLINDRICAL REGION OF RADIUS 2μm), CALCULATED BY THE METHOD DESCRIBED IN [2] AND BY THE PROPOSED ALGORITHM. THE TWO METHODS GIVE ESSENTIALLY THE SAME RESULTS.

computational efficiency, the proposed algorithm is expected to exhibit superior fidelity compared to standard timestep-based algorithms since it requires no timestep or spatial discretization.

Due to the non-interacting nature of deviational particles under this new formulation, the resulting mathematical and numerical descriptions share many similarities with their neutron trans-port counterparts. We expect the substantial literature on neutron transport and its simulation [11] to prove very useful towards improving the proposed method further.

REFERENCES
[1] Baker, L. L., and Hadjiconstantinou, N. G., 2005, "Variance reduction for Monte Carlo solutions of the Boltzmann equation", Phys. Fluids, **17**(5), 051703.
[2] Peraud, J.-P. M., and Hadjiconstantinou, N. G., 2011, "Efficient simulation of multidimensional phonon transport using energy-based variance-reduced Monte Carlo formulations", Phys. Rev. B, **84**(20), 205331.
[3] Wagner, W., 2008, "Deviational particle Monte Carlo for the Boltzmann equation", Monte Carlo Meth. Appl., **14**, 191.
[4] Radtke, G.A., and Hadjiconstantinou, N. G., 2009, "Variance-reduced particle simulation of the Boltzmann transport equation in the relaxation-time approximation", Phys. Rev. E, **79**(5), 056711.
[5] Hadjiconstantinou, N. G., Radtke, G. A., and Baker, L. L., 2010, "On Variance-Reduced Simulations of the Boltzmann Transport Equation for Small-Scale Heat Transfer Applications", J. Heat Transfer, **132**(11), 112401.
[6] Hao, Q., Chen, G., and Jeng, M.-S., 2009, "Frequency-dependent Monte Carlo simulations of phonon transport in two-dimensional porous silicon with aligned pores", J. Appl. Phys., *106*(11), 114321.
[7] Peterson, R. B., 1994, "Direct Simulation of Phonon-Mediated Heat Transfer in a Debye Crystal", J. Heat Transfer, **116**(4), pp 815-822.
[8] Mazumder, S., and Majumdar, A., 2001, "Monte Carlo study of phonon transport in solid thin films including dispersion and polarization", J. Heat Transfer, **123**(4), pp. 749-759.
[9] Lacroix, D., Joulain, K., and Lemonnier, D., 2005, "Monte Carlo transient phonon transport in silicon and germanium at nanoscales", Phys.Rev B, **72**(6), 064305.
[10] G. Chen, 2005, *Nanoscale Energy Transport and Conversion*, Oxford University Press, New York, Chap. 4.
[11] Spanier, J., and Gelbard, E. M., 1969, *Monte Carlo Principles and Neutron Transport Problems*, Addison-Wesley Publishing Company.
[12] Peraud, J.-P. M., and Hadjiconstantinou, N. G., 2012, "An

alternative approach to efficient simulation of small-scale phonon transport", *submitted to* Appl. Phys. Lett.

[13] Schmidt, A. J., Chen, X., and Chen, G., 2008, "Pulse accumulation, radial heat conduction, and anisotropic thermal conductivity in pump-probe transient thermoreflectance", Rev. Sci. Instrum., **79**(11), 114902.

[14] Minnich, A. J., Johnson, J. A., Schmidt, A. J., Esfarjani, K., Dresselhaus, M. S., Nelson, K. A., and Chen, G., 2011, "Thermal Conductivity Spectroscopy Technique to Measure Phonon Mean Free Paths", Phys. Rev. Lett., **107**(9), 095901.

[15] Minnich, A. J., 2011, "Exploring Electron and Phonon Transport at the Nanoscale for Thermoelectric Energy Conversion", Ph.D. thesis, Massachusetts Institute of Technology.

[16] Minnich, A. J., Chen, G., Mansoor, S., and Yilbas, B. S., 2011, "Quasiballistic heat transfer studied using the frequency-dependent Boltzmann transport equation", Phys. Rev. B, **84**(23), 235207.